Available online at www.sciencedirect.com
SCIENCE DIRECT®
Thermochimica Acta 421 (2004) 43–49
thermochimica acta
www.elsevier.com/locate/tca

Low frequency chain dynamic of cross-linked poly(acrylic acid)

Ch. Mayoux [a,*], J. Dandurand [b], C. Lacabanne [b]

[a] *SETARAM, 7 Rue de l'Oratoire, 69300 Caluire, France*
[b] *Laboratoire de Physique des Polymères., CIRIMAT, Université Paul Sabatier, 118 Route de Narbonne 31062 Toulouse Cedex 04, France*

Received 13 October 2003; received in revised form 13 February 2004; accepted 14 February 2004
Available online 8 May 2004

Abstract

Cross-linked poly(acrylic acid) (PAA) synthesized by radical polymerization in inverse suspension is a swelling gel. The physical structure of PAA has been analyzed using low frequency chain dynamic given by the analysis of thermo stimulated currents (TSC). The α primary dielectric relaxation mode observed around the glass transition temperature ($T_g = +38\,^{\circ}C$) corresponds to the slowest dynamic. The relaxation times of the constituting processes show that it is due to a delocalized cooperative molecular mobility involving nanometric sequences of the hydrocarbon skeleton. The β secondary dielectric relaxation mode observed at lower temperature ($T_\beta = -35\,^{\circ}C$) corresponds to a higher frequency molecular mobility. It has been assigned to the cooperative mobility of hydrogen bonded COOH groups. In fact, the hydrogen bonded side chains behave as an hydrophilic matrix in which nanometric domains constituted by sequences of the main chain are embedded. Such a picture might explain the specific swelling properties of cross-linked PAA.

Keywords: Poly(acrylic acid); Thermo stimulated currents; Dielectric relaxation; Glass transition; Molecular mobility

1. Introduction

Cross-linked poly(acrylic acid) (PAA) synthetized by radical polymerization in inverse suspension is well known for its ability to absorb an important amount of liquid [1]. This swelling property of cross-linked PAA is dependent upon several parameters such as temperature, solution pH [2], cross-linking ratio and beads morphology. Due to its specific property, this polymeric gel has found applications in different domains such as medicine, agriculture, construction, security, communication [3]. Despite the wide variety of applications, the molecular mechanism of swelling remains unclear.

The understanding of this macroscopic property implies a thorough analysis of the relationships between molecular mobility and structure. Among the techniques used to reveal them, we might cite nuclear magnetic resonance (NMR) [4], dynamic mechanical thermal analysis (DMTA), dynamic electrical thermal analysis (DETA) and thermo stimulated currents (TSC). This later one is particularly well suited to the analysis of local order that might be induced by molecular orientation in amorphous polymers [5]; it also allows us to distinguish the various phases in polyphasic amorphous materials [6]. The last but not least advantage of TSC is to be quite adaptable to the sample morphology. Consequently, TSC has been adapted for analyzing molecular mobility in cross-linked PAA in order to shed some light on the physical structure responsible for the swelling mechanism of PAA gel.

2. Experimental

2.1. Materials

Acrylic Acid (AA) was partially neutralized drop by drop by caustic solution (20%, w/w), kept cool to prevent the exothermic reaction and from AA precipitation. An aqueous phase was prepared by mixing neutralized AA, potassium persulfate ($K_2S_2O_8$) as the initiator and *N*,*N*′-methylene bisacryalmide (MBA_C) as cross-linking agent. To obtain the inverse suspension, this latter was introduced in an or-

* Corresponding author. Tel.: +33-4-7210-2594; fax: +33-4-7482-7176.
E-mail address: mayoux@setaram.com (Ch. Mayoux).

0040-6031/$ – see front matter © 2004 Elsevier B.V. All rights reserved.
doi:10.1016/j.tca.2004.02.024

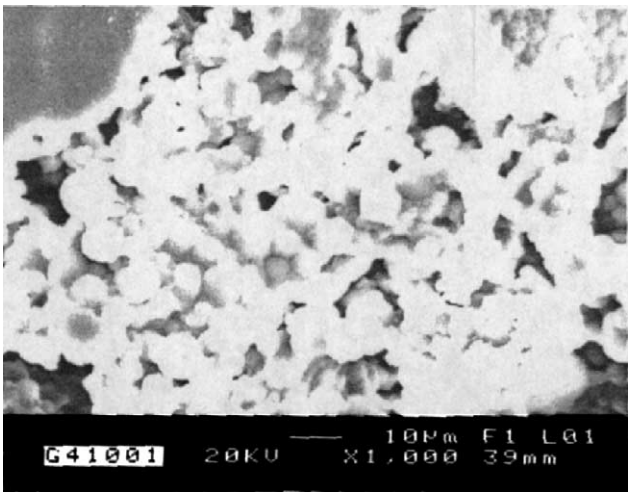

Fig. 1. Scanning electron microscopy of PAA beads (2–10 μm).

ganic one composed by heptane and SPAN 80 as surfactant [7]. Cross-linked PAA was recorded under beads shape after a methanol precipitation and drying under rough vacuum at 40 °C. The diameter of the beads was ranging from 20 to 13 μm. An example of particles observed through a scanning electron microscope (SEM) is shown in Fig. 1.

Note that, prior to TSC experiments, a thermal treatment was performed in order to erase any thermodynamic history. The glass transition temperature has been measured by Differential scanning calorimetry at a rate of 20 °C/min: in those conditions, we obtained $T_g = 38$°C [8].

2.2. Methods

Although this technique has been applied to the study of polymers in the seventies [9], we will recall briefly its principle. For recording a complex spectrum, the sample is inserted into a parallel plate capacitor, and it is subjected to a static electrical field (100 V/mm) at a polarization temperature T_p for a time t_p. The dipolar units present in the material and mobile at this temperature T_p can be oriented. In order to freeze this dipolar orientation, the sample is quenched to a temperature $T_0 \ll T_p$ and then the field is removed. Finally, the sample is heated at a constant rate $r = 7$ °C/min., while the depolarization current is recorded versus the temperature, constituting the complex TSC spectrum. In polymers, complex TSC spectra only give qualitative information. The analysis of the relaxation behavior implies to resolve complex TSC spectra into elementary components.

For obtaining elementary spectra, the procedure of fractional polarizations can be used. The sample is polarized at a temperature T_p ($E = 100$ V/mm) for a duration $t_p = 2$ min in order to orientate the dipolar entities having a relaxation time $\tau(T_p)$ lower than t_p. The temperature is then decreased till T_d ($T_d = T_p - \Delta T$) and the field is cut off. The temperature is maintained constant for a duration t_p in order to randomize the dipolar entities having a relaxation time $\tau < \tau$ (T_d) and finally, the dipolar orientation is quenched to T_0 The elementary spectra are recorded, following the same procedure than for the complex spectra. In this study, $\Delta T = 5$ °C. The elementary spectra are recorded following the same procedure than for the complex spectra. By shifting this polarization window [T_p, T_d] along the temperature axis by steps of ΔT, we obtain the complex spectrum decomposition in a series of elementary processes. With the above cited experimental parameters, elementary spectra are well described in the hypothesis of a Debye relaxation time.

3. Results and discussion

3.1. Secondary relaxation mode

For recording the complex TSC spectra of PAA, the polarization field was applied at 60 °C and the depolarization current was recorded in the temperature range from −160 to 100 °C. We present here the complex spectra obtained only in the low temperature range (−75, −20 °C) (Fig. 2). From −55 °C, the depolarization current increases to reach a maximum of some 0.2 pA at −35 °C. Considering the temperature position of this TSC peak, well below the glass transition temperature, it has been designated as a secondary relaxation mode, despite a rather high intensity.

In the literature, a lot of work has been devoted to the study of the low temperature molecular mobility of polymers like poly (vinyl acrylate) or poly (methacrylate), involving the ester group COOR and the influence of the chemical structure of the side chain has been analyzed [10–15]; this ester group can rotate around the C–C bond [4] linked to the main chain. Vanderschueren [16] investigated in poly (methylmethacrylate) and poly (ethylmethacrylate) the TSC β secondary relaxation mode strongly plasticized by water. This latter phenomena is well understood and explained because this molecular mobility involved polar groups. The origin of those secondary TSC modes has also been discussed by Van Turnhout [17]. In the case of the cross-linked

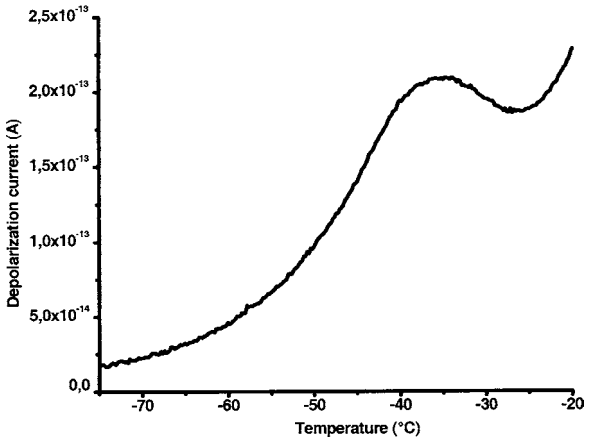

Fig. 2. Complex TSC spectrum of β secondary relaxation mode for cross-linked PAA. $E = 100$ V/mm.

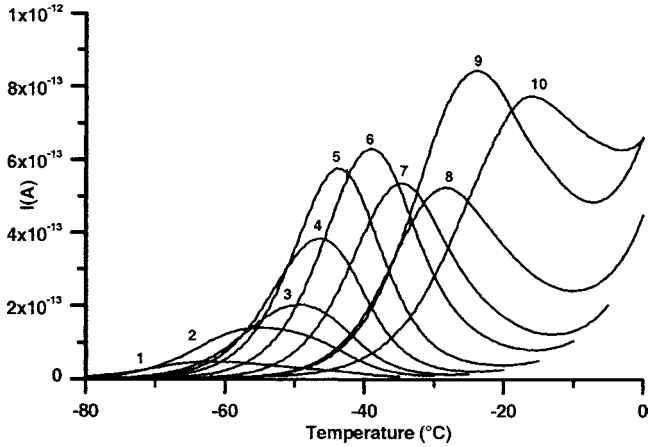

Fig. 3. Elementary TSC spectra constituting the β secondary relaxation mode for cross-linked PAA.

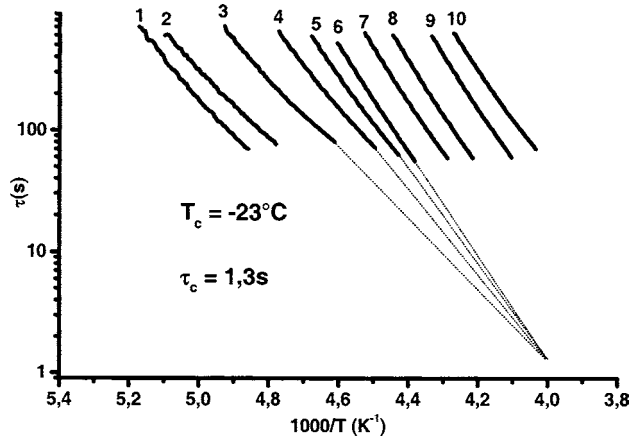

Fig. 4. Arrhenius diagram of relaxation times τ of the β secondary relaxation mode For cross-linked PAA.

PAA and concerning the β relaxation process, TSC experiments have allowed us to determine its temperature and to study its sensitivity to water (this latter work will be the subject of an other publication). Results obtained are in accordance with the literature, therefore, we can attributed this mode to the molecular mobility of the side chain COOH. Among secondary relaxation processes, the β mode of PAA distinguishes itself by a relatively high intensity that might be explained by the strong dipolar moment of the COOH group. As mentioned in the experimental part, we have used the fractionnal polarization procedure to analyze the complex spectrum. By shifting the polarization window ($\Delta T = 5\,^{\circ}$C) y steps of 5 °C in the temperature range (−80, 0 °C), we obtain the series of elementary processes represented on Fig. 3. The numbers indicate the order of happening for increasing polarization temperatures. Note that the envelop of elementary spectra practically reproduces the complex spectra (cf Fig. 2). Each elementary spectrum being practically described by the hypothesis of a single relaxation time, the dipolar relaxation P obeys a first order kinetic equation:

$$\frac{\mathrm{d}P(t)}{\mathrm{d}t} + \frac{P}{\tau T} = 0$$

The dielectric relaxation time $\tau(T)$ is given by

$$\tau(T) = \frac{P}{\mathrm{d}P/\mathrm{d}t} \tag{1}$$

The polarization $P(T)$ is deduced from the measured depolarization current $I(T)$.

$$I(T) = -sq\left(\frac{\mathrm{d}P(T)}{\mathrm{d}T}\right)$$

where s is the surface sample and q is the heating rate.

Then, the temperature dependence of relaxation times $\tau(T)$ can be calculated from Eq. (1), in the temperature range where the depolarization current is recorded. The logarithmic variation of these relaxation times has been plotted versus the reciprocal temperature for each elementary spectrum, on an Arrhenius diagram (Fig. 4). The experimental points follow straight lines reflecting that the relaxation times obey an Arrhenius equation:

$$\tau(T) = \tau_0 \exp\left(\frac{\Delta H}{RT}\right)$$

where ΔH is the activation enthalpy, τ_0 is the pre-exponential factor and R is the perfect gas constant. A linear regression allows us to reach the activation parameters. The activation entropy, ΔS has been extracted from the pre-exponential factor using the Eyring equation

$$\tau_0 = \frac{h}{k_{\mathrm{B}}T} \exp\left(\frac{\Delta S}{R}\right)$$

where k_{B} is the Boltzmann's constant, and h is the Planck's constant.

For each relaxation time we plot the semi-logarithmic variations of the pre-exponential factor To versus the activation enthalpy ΔH (Fig. 5). We can see that some experimental points (τ_0; ΔH) (points 3, 4, 5 and 6) are

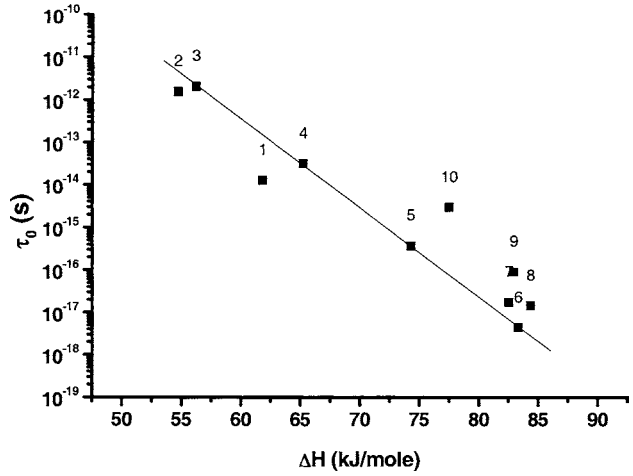

Fig. 5. Compensation diagram of the β secondary relaxation mode for cross-linked PAA.

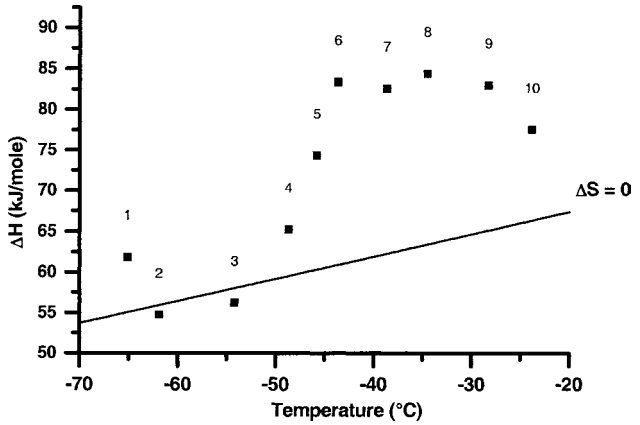

Fig. 6. Variation of activation enthalpy ΔH of secondary relaxation mode β vs. temperature for cross-linked PAA and Starkweather line for $\Delta S = 0$.

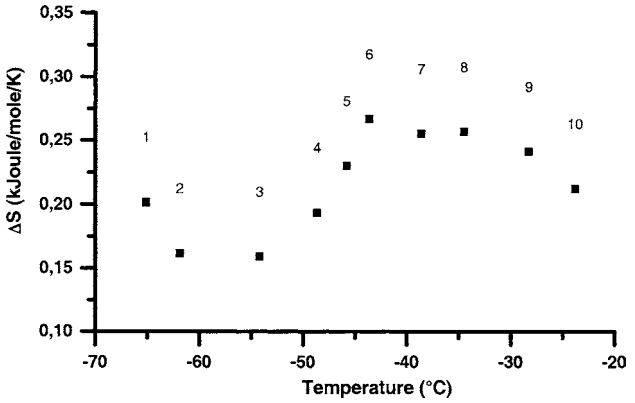

Fig. 7. Variation of activation entropy ΔS of secondary relaxation mode β vs. temperature for cross-linked PAA.

situated on a single line revealing the existence of a compensation law:

$$\tau_0 = \tau_C \exp\left(\frac{\Delta H}{RT_c}\right) \quad (2)$$

where τ_C is the compensation time and T_c is the compensation temperature.

The compensation temperature we have found, $T_c = -23\,^{\circ}C$ ($\pm 3\,^{\circ}C$), is, as usually, quite close from the one corresponding to the maximum of the global spectrum ($-35\,^{\circ}C$). The atypical value, for a secondary mode, of the compensation time, $\tau_C = 1.3\,s$ ($\pm 0.1\,s$), is generally found for primary relaxation modes. In Fig. 6, we present the variation of activation enthalpy versus temperature and the Starkweather's line [18] associated with a null activation entropy. Those activation enthalpy values correspond to the barrier for these side chain movements. From $-50\,^{\circ}C$, instead of following the Starkweather's line, the experimental points reach a maximum at $-37\,^{\circ}C$. This behavior reveals a cooperative character of the COOH groups movements. According to the Hoffman–Williams–Passaglia model [19], these activation energies are increasing linearly with the size of the mobile sequences. Here, we can consider that the morphology of PAA beads and the tri-dimensional network architecture allow the polar side chains to transfer the movement from one acid group to another hydrogen bonded one, even if they are quite far or in neighboring beads. As shown on Fig. 7, activation entropies are particularly high reflecting a high number of accessible sites for the mobile entities; it is a case where the thermodynamic parameters are relevant for understanding the physical structure of the environment of mobile dipoles [20]. Fixed onto the hydrocarbon backbone by only one end, the side chains are free to adopt different conformations in a matrix stabilized by hydrogen bonded COOH groups and water molecules. Cooperative molecular movements of such a matrix explains the dielectric response we observe. By its cooperative character and slow dynamic, this β secondary relaxation mode presents a transitional character even if no thermal event is found in the corresponding temperature range, by Differential Scanning Calorimetry.

3.2. Primary relaxation mode

We present in Fig. 8, the variation of the depolarization current versus temperature for cross-linked PAA, in the temperature ranging from (-150, $50\,^{\circ}C$), for polarization conditions indicated in the preceding paragraph. The β secondary relaxation mode is of course, always observed at the same temperature, i.e. $-35\,^{\circ}C$ and an additional primary mode is recorded. Since this primary mode is situated in the temperature range of the glass transition temperature T_g as measured from Differential Scanning Calorimetry, [8], it has been assigned to the dielectric manifestation of the glass transition.

In this temperature range, the conductivity phenomenon is responsible for a high temperature tail, not shown in Fig. 8, since the polarization temperature was moderate, but it should prevent any analysis of the fine structure by using fractional polarization. We avoid it by inserting a thin film of polypropylene (20 μm) between the electrode and the surface of the sample, this film plays the role of a

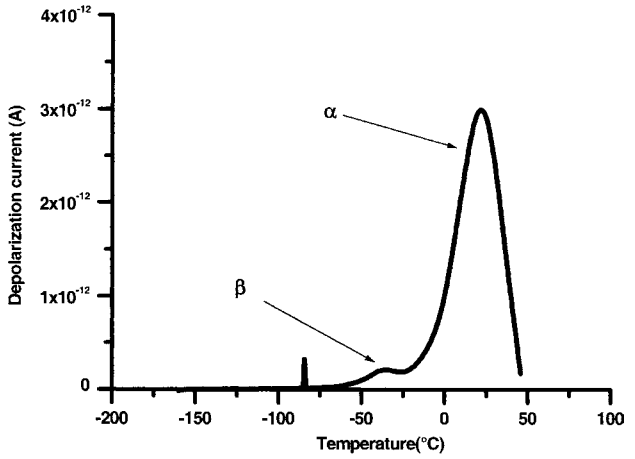

Fig. 8. Complex TSC spectrum of primary relaxation mode α for cross-linked PAA. $E = 100\,V/mm$.

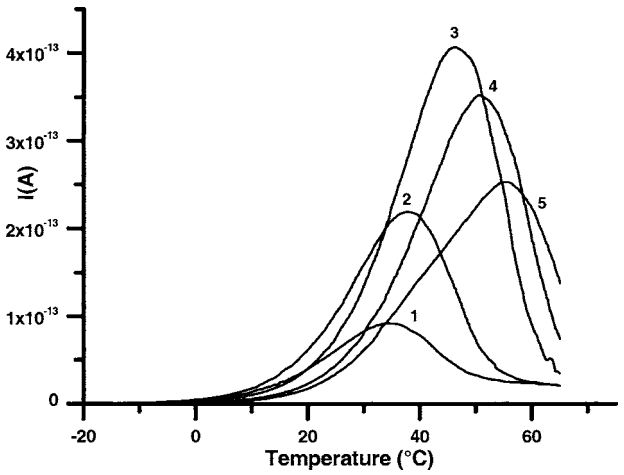

Fig. 9. Elementary TSC spectra from the α primary relaxation mode for cross-linked PAA obtained with the blocking electrode (polypropylene film).

blocking electrode. The elementary processes represented in Fig. 9 were obtained by shifting the polarization window ($\Delta T = 5\,^{\circ}$C) by steps of 5° in the temperature range from 0 to 70 °C. The envelop of these spectra is situated at higher temperature than the complex spectrum since the exploration has been extended towards higher temperatures.

In Fig. 10, the Arrhenius diagram shows the variation of relaxation times versus reciprocal temperature for cross-linked PAA. We can retain that this primary mode presents a narrow distribution of the relaxation times in comparison with the one of the secondary one.

Moreover, a quasi-linear behavior of these relaxation times is observed reflecting that the temperature dependence obeys an Arrhenius equation (Eq. (1)). This behavior is perfectly explained by the fact that, due to the very low equivalent frequency of TSC, the α primary relaxation mode is still observed in the vitreous state of PAA contrarily with previous dielectric experiments [21,22]. Moreover, we observe that some of these lines converge towards a compensation point ($T_c = 46\,^{\circ}$C ($\pm 3\,^{\circ}$C), $\tau_c = 1.5$ s (± 0.1 s) so that the relaxation times are well described by Eq. (2). This behavior is confirmed by the semi-logarithmic variation of τ_0 versus ΔH for involved processes which is linear as shown in Fig. 11. Despite the controversy on the relevance of compensation parameters associated with the primary relaxation mode [23], we have compared the compensation temperature T_c with the glass transition temperature T_g, $T_c - T_g = +8\,^{\circ}$C. Such a gap is coherent with the ones reported in amorphous polymers [24]—it is, for example, comparable with the one of syndiotactic PMMA [25]. So, the value recorded for PAA is perfectly sound according to its chain flexibility. Moreover, the compensation time, of the order of the second, is in good agreement with those found in the literature [20]. In order to confirm the cooperativity of this mode, we have reported in Fig. 12, the variation of the activation enthalpy versus temperature and the Starkweather's line [26]. Experimental points depart from this line, reflecting the cooperative character of this molecular mobility. Nevertheless, these values are lower than those classically recorded in the case of a primary relaxation mode. This cannot be only explained by the flexibility of the polymeric chain but it might also indicate that the mobile sequences are shorter. It is interesting to note that the flat maximum is in the region of the glass transition temperature: such a behavior has been reported for a wide variety of polymers [27]. The cooperative delocalized molecular movements revealed by this primary relaxation mode might be associated with the mobility of nanometric sequences of the hydrocarbon chains that segregate into domains that have the classical dielectric and calorimetric response of a thermoplastic. The peculiar swelling properties of PAA might be attributed to the existence of the hydrogen bonded matrix constituted by side chains and eventually water molecules. The cohesion

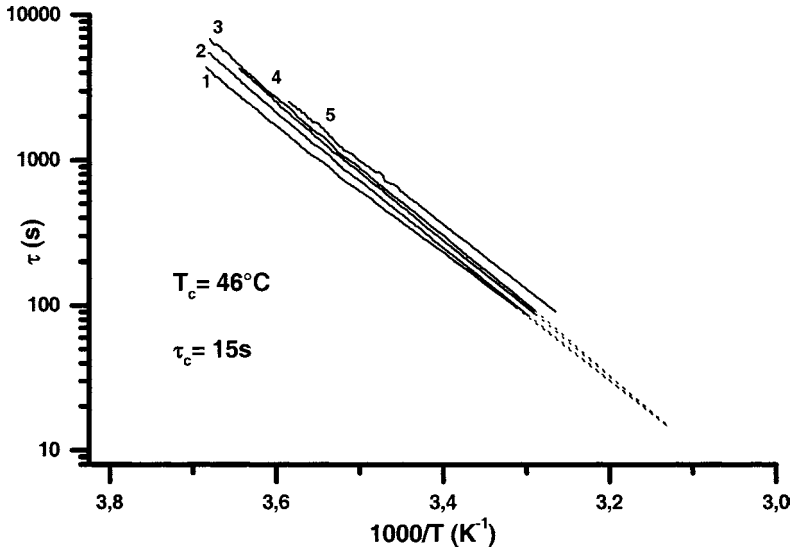

Fig. 10. Arrhenius diagram of relaxation times τ of the primary relaxation mode α for cross-linked PAA.

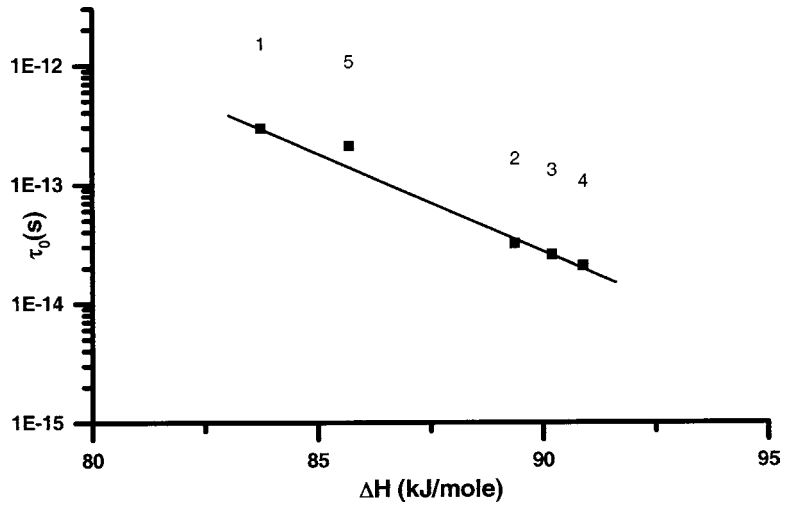

Fig. 11. Compensation diagram of the primary relaxation mode α for cross-linked PAA.

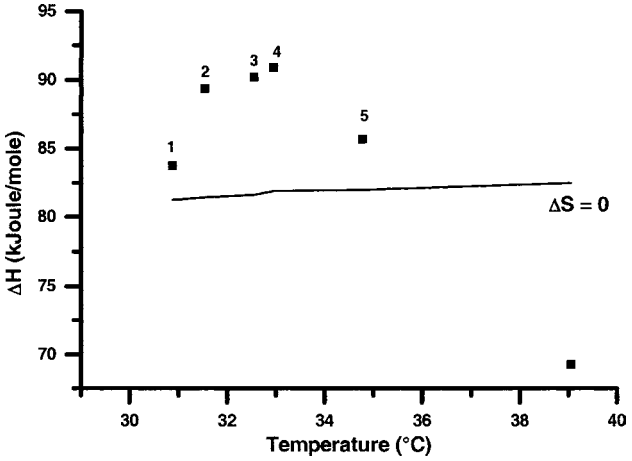

Fig. 12. Variation of activation enthalpy ΔH of α primary relaxation mode versus temperature for cross-linked PAA and Starkweather line for $\Delta S = 0$.

of this swelling matrix is ensured by the hard hydrocarbon domains.

4. Conclusion

The molecular mobility of PAA has been explored by Thermo Stimulated Currents. At low temperature, around −35 °C, a secondary relaxation mode is observed. This mode is very sensitive to the presence of water molecules so that it might involve COOH groups. It is constituted of elementary processes with relaxation times following a compensation equation, with a compensation time of the order of the second. Considering this behavior law and its relatively high intensity, this mode has been attributed to delocalized cooperative movements of side chains constituting a hydrogen bonded matrix.

In the vicinity of the glass transition temperature (38 °C), a primary relaxation mode is observed. It can be described by a distribution of relaxation times following a compensation law with compensation parameters that indicates that it is associated with the glass transition. Then, it has been assigned to the delocalized cooperative movements of nanometric main chains sequences.

This dielectric response of cross-linked PAA gel suggests the existence of a biphasic structure with hard hydrocarbon domains embedded in a soft matrix constituted by hydrogen bonded side chains. Such a physical structure might explain the swelling properties of cross-linked PAA.

References

[1] A.M. Degouw, J. Prins, J. Dingermans, European Patent Application, EP 68,530 (1983).
[2] F.L Buchhloz, N.A. Peppas, Superabsorbent Polymers, series 573, ACS, 1994, Washington, DC, pp. 27–35.
[3] H. Polle, European Patent, EP 375,685 (1990).
[4] K. Schmidt-Rohr, A.S. Kulik, H.W. Beckham, A. Ohlemacher, U. Pawelzik, C. Boeffel, H.W. Spiess, Macromolecules 27 (1994) 4733–4745.
[5] E. Dudognon, A. Bernès, C. Lacabanne, Polymer 43 (2000) 5175–5179.
[6] H.S. Faruque, C. Lacabanne, Polymer 27 (1986) 527–531.
[7] C. Mayoux, J. Dandurand, A. Ricard, C. Lacabanne, J. Appl. Polym. Sci. 77 (2000) 2621–2630.
[8] C. Mayoux, Paul Sabatier University PhD Thesis 2000 (Chapter 4).
[9] C. Lacabanne, D. Chatain, J. Polym. Sci.–Phys. Ed. 11 (1973) 2315–2328.
[10] G.P. Mikhailov, T. Borisova, Vysokomol. Soed. 2 (1960) 177.
[11] J.N.G. McCrum, B.E. Read, G. Williams, Anelastic and Dielectric Effects in Polymeric Solids, Wiley, New York, 1967 (reprinted by Dover, New York, 1991).
[12] P. Hedvig, Dielectric Spectroscopy of Polymers, Adam Hilger, Bristol, 1977.
[13] J.P. Runt, J.J. Fitzgerald, Dielectric Spectroscopy of Polymeric Materials, ACS, Washington, DC, 1997.

[14] I.M. Ward, Mechanical Properties of Solid Polymers, Wiley, London, 1971.
[15] M. Randak, V. Adamec, Plaste. Kautsch. 19 (1972) 905–912.
[16] J. Vanderschueren, A. Linkens, Macromolecules 11 (1978) 1228–1235.
[17] J. Van Turnhout, Polymer 2 (1971) 173–181.
[18] H.W. Starkweather, Macromecules 14 (1981) 1277–1281.
[19] J.D. Hoffman, G. Williams, E.J. Passaglia, Polym. Sci. C14 (1996) 173–235.
[20] K. Shibayama, Y. Suzuki, Polym. Sci. 3 (1965) 2637–2643.
[21] N.F. Shepard, J.R. Senturia, S.D. Senturia, J. Polym. Sci. 27 (1989) 753–762.
[22] J.P. Crine, J. Macromol. Sci. B23 (1984) 201–219.
[23] B. Sauer, J.J. Moura Ramos, Polymer 38 (1997) 4065–4069.
[24] C. Lacabanne, A. Lamure, G. Teyssèdre, A. Bernès, M. Mourgues, J. Non Crystall. Solids 172–174 (1994) 884–890.
[25] S. Doulut, C. Bacharan, P. Demont, A. Bernès, C. Lacabanne, J. Non Crystall. Solids 235–237 (1998) 645–651.
[26] H.W. Starkweather, Macromolecules 14 (1981) 1277–1289.
[27] E. Dantras, E. Dudognon, V. Samouillan, J. Menegotto, A. Bernès, P. Demont, C. Lacabanne, J. Non Crystalline Solids 307–310 (2002) 671–678.